Resonant inelastic x-ray scattering of curium oxide

K. O. Kvashnina,[1,*] S. M. Butorin,[1] D. K. Shuh,[2] J.-H. Guo,[3] L. Werme,[1,4] and J. Nordgren[1]
[1]*Department of Physics, Uppsala University, Box 530, 751 21 Uppsala, Sweden*
[2]*Chemical Sciences Division, Lawrence Berkeley National Laboratory, Berkeley, California 94720, USA*
[3]*Advanced Light Source, Lawrence Berkeley National Laboratory, Berkeley, California 94720, USA*
[4]*SKB, Stockholm, Sweden*
(Received 9 August 2006; revised manuscript received 29 January 2007; published 8 March 2007)

The measurements on radioactive actinide isotopes (curium-248) were performed using very small sample quantities (micrograms) to minimize the sample activity. Resonant inelastic x-ray scattering (RIXS) spectra of curium oxide at the Cm 5*d* edge were measured for the first time. RIXS data are compared with theoretical calculations using atomic multiplet theory. The results indicate that isotope curium −248 in the curium oxide sample has oxidation state III due to the best agreement with RIXS calculations for Cm (III) instead of those for Cm (IV).

DOI: 10.1103/PhysRevB.75.115107 PACS number(s): 25.30.Dh, 21.60.Jz, 25.20.Dc, 25.55.Ci

INTRODUCTION

Since the discovery of the transuranium elements there has been a continuing interest in determining the chemical and physical properties of these elements and their compounds. In particular, it was necessary to determine the chemistry of plutonium and neptunium very accurately because of the requirements for separation and purification of $_{94}Pu^{239}$ from the other materials in uranium piles. As a result of this, it is now stated that the chemistry of plutonium is as well or better understood than that of other actinides in the periodic table. Recently, the electronic structure of actinides has been studied using different experimental and theoretical approaches.[1–4]

Uranium has the valence states (III), (IV), and (VI), while neptunium and plutonium have the valencies (III), (IV), (V), and (VI). However, greater oxidizing power is required to oxidize them to their higher states.[5] The stability of the valence state of (III) increases from uranium to plutonium and it is predicted that maximum stability could probably be obtained with curium (element 96), which has seven 5*f* electrons. The known properties of these transuranium elements make it possible to suggest a subclassification of these elements in terms of a new series similar to the rare earth series. The electronic configuration explains satisfactorily the stable valence state of (III) for gadolinium, which compares with the state of (III) for curium. This prediction is also verified by data, which indicate that spin polarization of the curium 5*f* electrons stabilizes the curium (III) valency.[5]

In the case of curium, there are still numerous open questions ranging from the crystal structure[6] and magnetic properties[7] of curium compounds to the research of the nature of curium ions in various oxidation states. It is, therefore, important to investigate the electronic structure of curium in different oxidation states.

A theoretical study of curium compounds is an additional source for obtaining chemical and structural information, but this entails a mixture of success and difficulties as for other *f* elements. The most commonly used are the density function theory (DFT) and *ab initio* calculations,[2] which have been shown to be sufficient to describe crystal structures with various types of chemical bonding: halides, pnictides, hydrides, and oxides of curium.[6,8,9] Recently, relativistic calculations using the Dirac-Slater discrete variational method (DVM) has been carried out in order to obtain the electronic structure of curium fluorides and chlorides.[10] Curium(III) oxide has been studied using Dirac-Hartree-Fock calculations, which provided information about the curium-oxygen distance in the model of hydrated Cm(III).[11] Using the same theoretical approach, curium fluorides in different valencies from (I) to (IV) were compared to gadolinium fluorides. Since CmF_4 has been successfully prepared[12] whereas GdF_4 has not yet been possible to synthesize, it was concluded that $5f^7$ in CmF_3 is less stable than $4f^7$ in GdF_3.[13]

Most of the theoretical investigations of curium have been performed in comparison with gadolinium due to their similar electronic configuration. Optical absorption and selective laser excitation spectroscopy have been used to investigate the electronic structures of the Cm(III) and Gd(III) ions in host crystals of $LuPO_4$, and these two systems were compared.[14] We also would like to mention that not so many experimental investigations have been found in the literature for curium compounds. Mostly these two types of spectroscopy have been used for curium.[15–17] A few more reports on laser-induced fluorescence (LIF) spectroscopy have also been written and this technique was proposed to test curium leaks from waste storage sites into groundwater[18] (REF3Mouchizuki). Later LIF was also applied to evaluate the water hydration number in the first shell around the Cm(III) ion.[19] Some experimental data on aqueous Cm(III) solution are available, but the electronic structure is not clear yet.

The radioactivity of curium makes it difficult to investigate all aspects in detail. Information on electronic properties obtained from theoretical calculations is helpful in analyzing experimental data. We report here resonant inelastic x-ray scattering (RIXS) of curium oxide near 5*d* edge. RIXS measurements at the actinide 5d threshold have been performed before[3,4] and provided high resolution, which makes it easier to study in detail elementary excitations in curium compounds. The technique is sensitive to the oxidation state and the speciation of curium contrasting to x-ray absorption spectroscopy (XAS) where the 5*d* core-hole lifetime broad-

ening is large. As a result, the actinide 5d absorption spectra do not exhibit many sharp features,[3,4] thus reducing the utility of XAS. In particular, it is difficult to distinguish between uranium species with different oxidation states, especially in the case when one of the species has a much lower concentration than another. The superlative resolution (defined by the response function of the instrument) of the RIXS technique and its ability to enhance transitions to low-lying excited states makes this technique especially powerful.

Experimental data was interpreted by the commonly used atomic multiplet theory based on the Hartree-Fock calculations. Sugar first presented the details of these types of calculations.[20] Later it was repeated and used in theoretical studies of most of the rare-earths metals, oxides, and chlorides. The theoretical calculations of curium oxides presented in that paper have been done in the same way as a previous one for gadolinium.[21] Comparison of experimental data with theoretical calculations for Cm(III) and Cm(IV) indicates that isotope curium-248 as curium oxide has oxidation state (III), which is quite similar to the observation of valency stability in the lanthanide series.

EXPERIMENTAL RESULTS

The oxidized curium-248 sample used for the measurements was fabricated by standard techniques used to prepare radionuclide counting plates. The counting plate was prepared from an aqueous solution of about 0.5 mM curium-248 in approximately 0.1 M HCl that was localized onto the surface of high purity platinum substrate (25.4 mm diameter, 0.05 mm thickness) by successive, partial micropipette aliquots into an area of about 4 mm^2. The isotopic composition of the curium solution was determined by α spectroscopy to be about 97% curium-248 and 3% curium-246 by mass.

The aqueous solution was allowed to dry and the resulting solid residue was distributed in a ring-shaped manner. This structure was inductively heated to 700 °C under atmosphere to oxidize the material and to fix the material onto the substrate to preclude loss in the UHV spectrometer chamber during the measurements. The final amount of Cm-248 on the counting plate was found to be about 2 μg possessing less than 20 nanocuries of activity.

For Cm, at temperature 600–800 °C the oxide that will initially form is a body-centered cubic (bcc) oxide with a stoichiometry of Cm=1 and an oxygen content of O =1.5–1.7. This supports an oxide with the general formula of $CmO_{1.5-1.7}$. As this Cm oxide was prepared from an acidic solution with chloride present and was to oxidize by 700 °C heating, this should lead to more stoichiometric ratio as $Cm_2O_{3.2}$, which might contain up to 10% of Cm (IV).

However at this high temperature there is also the possibility of forming a ternary Cm-Pt-O phase when this is performed on a Pt substrate. The bcc phase can be the precursor to Cm_7O_{12} which is a black, difficult to form stable phase with a Cm (IV) of up to 40%. This phase is favored by a slow quench to room temperature, whereas the material used in this experiment underwent a rapid quench. Direct examination by a visible microscopy of the materials, although it is a tiny amount on the surface, shows no evidence of a black material.

The portion of the platinum counting plate containing the curium was cut into a 3 mm×3 mm square and mounted with conductive tape on a rectangular aluminum sample holder. This sample holder was then inserted into a slotted aluminum can which served as a catch tray for material that might come loose during handling and the measurements.

The experiments were made at beamline 7.0 of the Advanced Light Source, Lawrence Berkeley National Laboratory, USA.[22] This undulator beamline includes a spherical grating monochromator, which gives resolution of 50 meV at ~110 eV. Absorption spectra at the Cm 5*d* edge were recorded by measuring the total electron yield (TEY) with 0.2 eV monochromator resolution at 110 eV. RIXS spectra were recorded using a grazing incident grating spectrometer[23,24] with 110 meV resolution at 120 eV. The instrument has three gratings, mounted at fixed angles of incidence and a large two-dimensional multichannel detector. The incident angle of the photon beam was 20° from the surface for solid samples and the spectrometer was placed in the horizontal plane at an angle 90° with respect to the incident beam.

RIXS measurements at the actinides 5*d* threshold provide an opportunity to study in detail elementary excitations in actinide compounds due to the naturally higher resolution of such experiments in comparison with those at the actinide 3*d* and 4*d* threshold. Normalized x-ray absorption (XA) and RIXS spectra at the Cm 5*d* edge measured for the curium-248 isotope is in the oxide sample are shown in Fig. 1. The absorption spectra show the pre-edge around 116 eV and the "giant resonance"[25] regions. Note that small spectral structures observed at energies of somewhat lower than 110 eV are likely due to the Pt 4*d* absorption edge in third order. The lettered arrows in Fig. 1 correspond to the excitation energies at which the scattering spectra were measured. RIXS spectra of curium were also taken at an incident photon energy below, at, and above the 5*d* "giant resonance." The RIXS intensity is plotted on the energy-loss scale. All the RIXS spectra are dominated by the elastic peak and the observed inelastic profiles for Cm (Fig. 1) show a multiplet family at about 2–4 eV below the elastic peak.

When the incident photon energy *a* is on the low-energy side of the pre-edge structure, we have extremely weak inelastic features, which show some similarity to RIXS profiles in the spectra recorded at excitation energies *b*-*i*. When the excitation energy is tuned to the peak *b*, the inelastic features appear. The energy difference between the elastic peak and inelastic scattering structures are listed in Table II. Similar profiles are observed for excitation energies *c* and *d*. A resonance is encountered upon tuning the incident energy to the energy *d* and to energies of the giant absorption edge (*e*, *f*, *g*, *h*, *and i*). At the excitation energy higher than the *i* resonance in the absorption curve, the relative RIXS contribution becomes weaker. A similar effect was observed for uranium in RIXS spectra across the 5*d* edge.[3,4] All inelastic features are clearly seen in all spectra but the intensity of the features strongly depended on excitation energy. Thus, the intensity for the feature at about −2.1 eV below the elastic peak goes up at the excitation energies *b and c*, and reached a maximum at the excitation energy *d*. When the incident photon energy is tuned to the giant resonance region in the absorp-

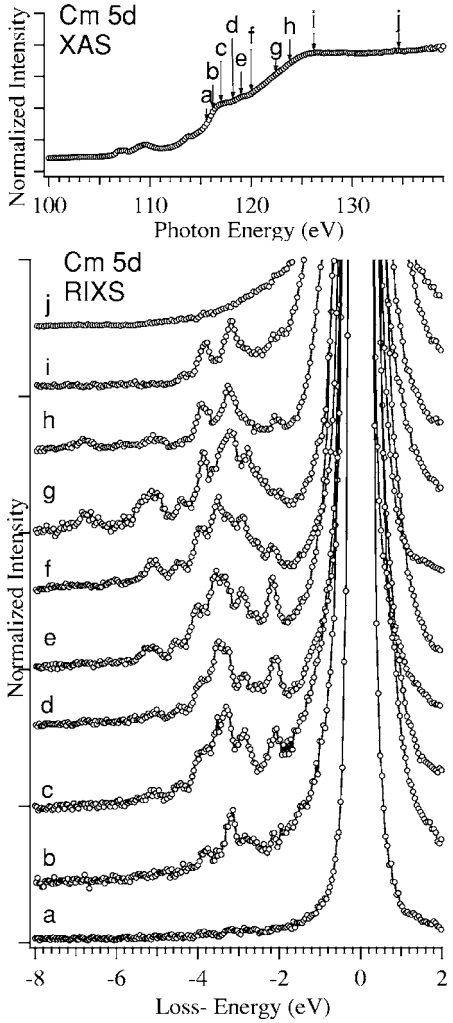

FIG. 1. Cm 5*d* XAS (top panel) and RIXS spectra across the 5*d* edge plotted on the energy-loss scale. The elastic peak is set to 0 eV. Excitations energies *a*-*l* are indicated by lettered arrows on the XA spectrum.

tion curve, this inelastic structure became weak (at excitation energies *e*, *f*, *g*, *h*, and *i*). The opposite effect is observed for the feature at about −3.9 eV below the elastic peak. At excitation energies below the giant resonance (*b*,*c*,*d*), this inelastic structure is quite weak and the intensity of this peak increases with the excitation energies *e*, *f*, *g*, *h*, and *i*. The calculation reproduces this effect fairly well and shows that these structures, corresponding to the *f*-*f* transitions strongly depend on the excitation energy and valency of the investigated actinide element.

THEORETICAL CALCULATIONS

The calculations were carried out for free (III) and (IV) ions of curium using atomic multiplet theory.[26] This approximation works quite well for describing rare-earth systems across 3*d* and 4*d* edges.[3,21,27,28] The 4*d*, 5*d*, and 5*f* shells for the actinide elements have similar general characteristics as the 3*d*, 4*d*, and 4*f* shells for the rare-earth elements. We expect that for the actinides, this approach will work as well.[3] XA spectra across 5*d* edge were already calculated by Ogasawara *et al.*[29] for most of the actinides, but they only treated trivalent ions, except Th (IV). In this paper we calculated the 5*d* XA and RIXS for Cm (III) and Cm (IV) ions.

TABLE I. Slater integrals and spin-orbit coupling constants used in model calculations.

Values	Cm (III)	Cm (IV)
$F^2_{(5f,5f)}$	7.97	8.90
$F^4_{(5f,5f)}$	5.21	5.85
$F^6_{(5f,5f)}$	3.82	4.31
$\zeta_{(5f)}$	0.39	0.42
$\zeta_{(5d)}$	4.31	4.34
$F^2_{(5d,5f)}$	8.88	9.12
$F^4_{(5d,5f)}$	5.74	5.99
$G^1_{(5d,5f)}$	9.34	9.74
$G^3_{(5d,5f)}$	5.78	6.05
$G^5_{(5d,5f)}$	4.13	4.32

The values for parameters such as Slater integrals and spin orbit coupling constants are obtained using Cowan's program.[26] The effect of crystal field or mixing with ligand bands was not taken into account. However, the effect of configuration interactions should be taken into account and is usually done by reducing the value of the Slater integrals. Lynch *et al.*[30] proposed that the Slater integrals for lanthanides should get smaller with increasing atomic number and will result in the broadening of the spectra.

The configuration of the outer electrons in curium is similar to that of gadolinium and has a half-filled 5*f* shell. The calculations of Cm 5*d* XA spectra were made in a similar way as for gadolinium,[21] where the Slater integrals $Fk(5f,5f)$ were reduced to 80%, and the $Fk(5d,5f)$ and $Gk(5d,5f)$ to 75% and 66%, respectively. Values of the Slater integrals and the spin-orbit coupling constants used for calculations of spectra are shown in Table I for the initial and final states of Cm (III) and Cm (IV). The configuration of the relevant outer electrons in Cm (III) is $5d^{10}5f^7$ and the half-

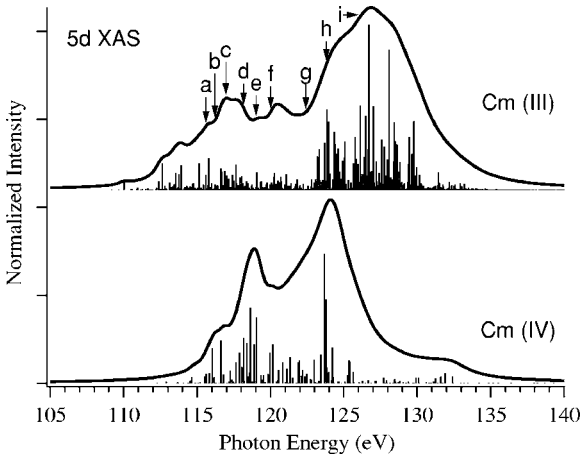

FIG. 2. Calculated 5*d* XA spectra of Cm (III) and Cm (IV) ions using atomic multiplet theory.

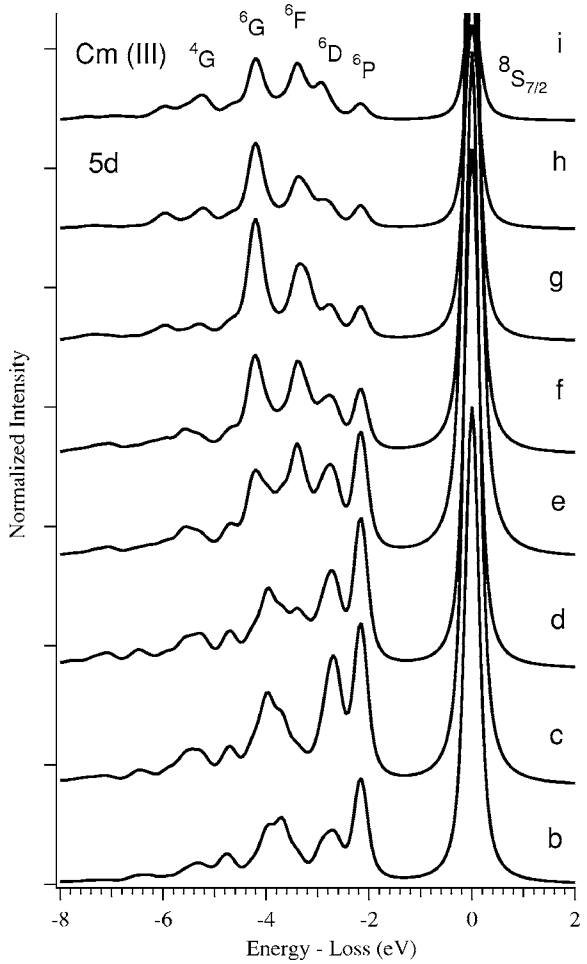

FIG. 3. Calculated 5*d* RIXS spectra of Cm (III) ion. Excitation energies are indicated in Fig. 2.

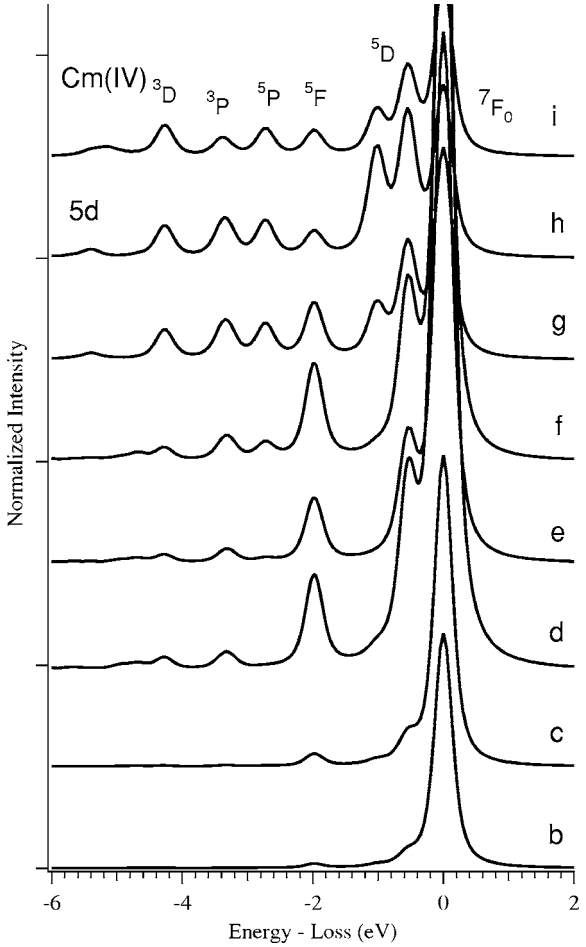

FIG. 4. Calculated 5*d* RIXS spectra of the Cm (IV) ion. Excitation energies are indicated in Fig. 2.

filled 5*f* shell produces, as a ground state, $^8S_{7/2}$. Thus, Cm (IV) has six electrons in the 5*f* shell, producing a $^7F_0$ ground state. The ground state *J* value is determined by Hund's rule. The final states have only three possibilities $J-1$, J, and $J+1$ and the dipole selection rules reduce the number of states that can be reached from ground state configuration, but it is still very large—Cm (III) has 1076 transitions and Cm (IV) has 212 transitions.

The calculated 5*d* XA spectra for Cm (III) and Cm (IV) are shown in Fig. 2. The plotted curves above the multiplet sticks are their Lorentzian convolutions. Both 5*d* XA spectra were divided in two regions: prethreshold and giant absorption region similar to the rare earth systems. The broadening width Γ for the prethreshold region was 1.0 eV and for the giant resonance region 2.5 eV. It was observed before by Richter *et al.*[31] for lanthanides that increasing the nuclear charge *Z* shifts all peaks towards higher energy. The XA spectrum for $_{96}$Cm (IV) should be similar to the $_{95}$Am (III) due to the same number of electrons in the *f* shell. Figure 2 clearly indicates the same effect for actinides as for lanthanides: the 5*d*-5*f* resonance for Cm (III) ($Z=96$) is shifted by 3 eV compared to Cm (IV) [as analog for Am (III) $Z=95$]. In order to achieve the best agreement between theory and experiment, the theoretical spectra for both ions were shifted towards lower energy by 5.8 eV, which is quite similar to the situation with Gd 4*d* XA spectrum where theoretical curve has been shifted by 6 eV (Ref. 31) for comparison with experiment.

The 5*d* RIXS spectra have been calculated from the Kramers-Heisenberg formula, using the matrix element in transitions from the ground state to the intermediate and back to the final states and using the same scaling for the Slater integrals as for gadolinium.[21] Figures 2 and 3 show the results for 5*d* RIXS of Cm (III) and Cm (IV) ions calculated for different excitation energies, which are exactly the same as used during the measurements of 5*d* RIXS spectra for curium oxide. The spectra are plotted on an energy-loss scale, where the elastic scattering is set to 0 eV and is clearly seen as dominant in all of the resonant spectra. The spectral structures at about 1–6 eV below the elastic peak represents the resonant inelastic x-ray scattering. The x-ray inelastic cross section was calculated using different values for the lifetime broadening in the intermediate state to simulate its significant increase in the giant resonance region.[32] The lifetime in the calculations of 5*d* RIXS spectra at excitation energies *b*, *c*, and *d* was set to 0.8 eV and 2.5 eV was used for the rest of the spectra. The plotted curves representing RIXS spectra are Voigt convolutions (combination of a Lorentzian with $\Gamma=0.2$ eV and a Gaussian with $\Gamma=0.2$ eV) of calculated multiplet sticks.

TABLE II. Energy difference between elastic peak and inelastic scattering structure ^5D, ^5F, ^5P, ^3P, ^3D for Cm (IV) and ^6P, ^6D, ^6F, ^6G, ^4G for Cm (III) in RIXS spectra across the 5*d* edge. Table also represents the energy difference between elastic and inelastic features in RIXS 5*d* experiments for Cm isotope in studied sample.

5*d* RIXS experiment	5*d* RIXS Cm (III)	(eV)	5*d* RIXS Cm (IV)	(eV)
−2.1	^{6}P	−2.1	^{5}D	−0.5
−2.8	^{6}D	−2.7	^{5}F	−2.0
−3.2	^{6}F	−3.4	^{5}P	−2.7
−3.9	^{6}G	−4.0	^{3}P	−3.3
−4.4	^{4}G	−4.7	^{3}D	−4.2

Generally two types of photon-in/photon-out features can be observed in all spectra—elastic and inelastic scattering. The inelastic scattering process of Cm (III) described by transitions from the ground state $^8S_{7/2}$ to the intermediate states of the $5d^95f^8$ configuration and then to the final states of the $5d^{10}5f^7$ configuration. The observed inelastic scattering profile for Cm (III) (Fig. 3) caused by transitions from the $^8S_{7/2}$ ground state to the final states ^6G_J, ^6F_J, ^6D_J, ^6P_J with different J values (according to selection rule), which are situated 2–4 eV below the elastic peak and then weaker transitions due to final state ^4G_J observed at 5 eV below the elastic peak. The observed inelastic scattering features for Cm (IV) (Fig. 4) caused by transitions from the $^7F_0$ ground state to final states ^5D_J, ^5F_J, ^5P_J, and weaker transitions due to the ^3P_J, ^3D_J final state terms. The energy differences between the elastic peak and inelastic scattering structures for Cm (III) and Cm (IV) are listed in Table II.

The inelastic scattering features for both ions are attributed to 5*f*-5*f* intra-atomic transitions (*f*-*f* excitations), which usually appear 1–2 eV below the elastic peak. By comparing the energies of the *f*-*f* excitations for calculated and experimental 5*d* RIXS spectra (Table II), it could be concluded that the energy separation between the elastic peak and the inelastic scattering structure for the Cm (III) ion is similar to that measured for the curium-248 isotope in the oxide sample and quite far from that for Cm (IV). A detailed comparison between the experimental results and the calculated spectra for the Cm (III) ion is given in the next section.

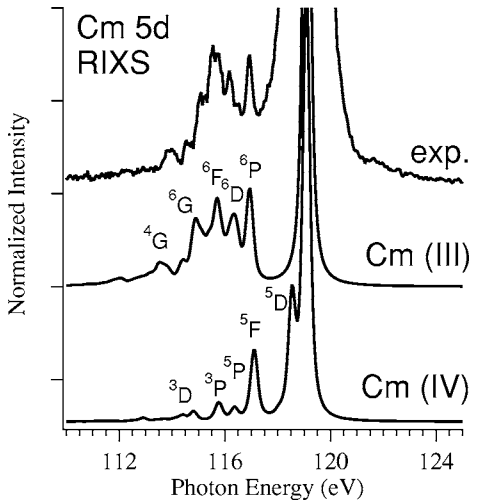

FIG. 5. Cm 5*d* RIXS of curium oxide taken at excitation energy of 119.0 eV and compared with calculated spectra for Cm (IV) and Cm (III) ions at the same excitation energy.

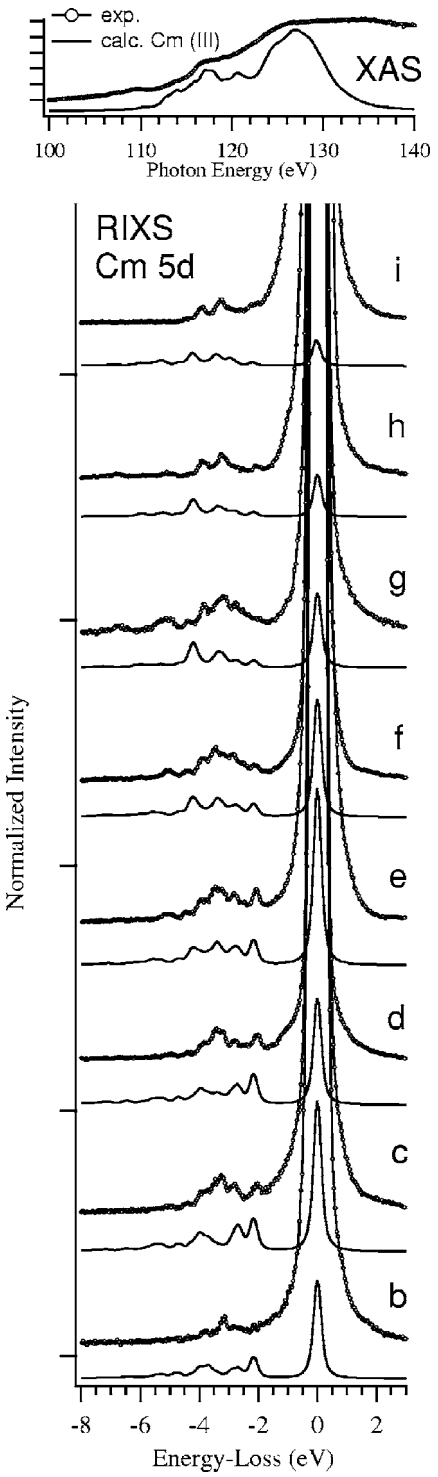

FIG. 6. Comparison between Cm 5*d* XAS and RIXS experimental data and calculated spectra for the Cm (III) ion. Excitation energies are the same as indicated in Fig. 1.

COMPARISON BETWEEN THEORY AND EXPERIMENT

Figure 5 shows the comparison of experimental data with theoretical calculations for the Cm (IV) and Cm (III) ions at excitation energy 119.0 eV, which is indicated by the lettered arrow *e* on the Cm 5*d* XA spectrum. The energy separation between the elastic peak and the inelastic scattering features in the calculated spectra for Cm (IV) and Cm (III) (Table III) allowed us to conclude that the curium-248 isotope had oxidation state (III) in the studied sample. This is supported by the dependence of the whole set of experimental data and calculated spectra for the Cm (III) ion on varying excitation energy (Fig. 6).

The calculated inelastic features in Cm (III) 5*d* RIXS show 5 main peaks due to the final state terms ^6G_J, ^6F_J, ^6D_J, ^6P_J, and ^4G_J, which appear at constant energy for varying excitation energies. Exactly the same profile appears in the experimental spectra for the curium oxide.

Generally the same tendency is observed for features ^6P_J and ^6G_J in the simulated and experimental spectra. When the incident photon energy is tuned to the giant resonance region of the absorption curve, the intense inelastic structure ^6P_J becomes weak (at excitation energies *e*, *f*, *g*, *h*, *and i*). The opposite behavior is observed for feature ^6G_J. At excitation energies below the giant resonance (*b*, *c*, *and d*) the inelastic structure ^6G_J is quite weak and the intensity of this peak increases with increasing excitation energies *e*, *f*, *g*, *h*, *and i*. This effect confirms the fact that the oxidation state of curium in the studied sample was (III). For the simulated 5*d* RIXS spectra of Cm (IV), we do not find similar dependence.

The experimental data for excitation energies *b* and *c* show a quite intense ^6F_J peak but the calculated spectra do not reproduce this peak. The peak is also not found pronounced at excitation energy *d* as compared with experiment, but its intensity starts to grow up. The feature ^6G_J is shifted 0.2 eV towards higher energy compared to experimental data as observed for excitation energies *e*, *f*, *g*, *h*, *and i*. The reason can be in applied uniform scaling of the F^2, F^4, and F^6 integrals, describing *f-f* interactions in our calculations while configuration interaction and hybridization with O 2*p* states may reduce these integrals differently.

Similar profile and excitation energy dependence observed for calculated and experimental RIXS spectra demonstrate that atomic multiplet theory is an appropriate tool for description of experimental results obtained for actinides system.

CONCLUSION

The data from this experiment is the first chemical information from a curium 5*d* edge obtained with a tunable photon source at a soft x-ray synchrotron radiation facility. The experimental results of the curium-248 isotope are interpreted using the atomic multiplet approach. This theory turns out to be very appropriate for actinide systems and demonstrates satisfactory agreement with experiment. Present RIXS data along with calculations provide valuable information on energies of intra-atomic *f-f* excitations in curium oxide. Comparison of experimental data with theoretical calculations for Cm(III) and Cm(IV) indicates that investigated curium-248 isotope has oxidation state (III) in the oxide sample which can in turn be concluded to be Cm_2O_3. This is in agreement with observation of valence stability in actinide series for actinide elements beyond plutonium.

The results of RIXS measurements have major implication for future studies. They show that microgram amounts of radioactive materials, which can be safely handled, is sufficient for detailed chemical and physical characterization of actinide compounds.

ACKNOWLEDGMENTS

This work was supported by the Swedish Nuclear Fuel and Waste Management Co. (SKB), by the Swedish Research Council, and Goran Gustafsson Foundation for Research in Natural Sciences and Medicine. The ALS work was supported by the Director, Office of Science, Office of Basic Energy Sciences, Division of Chemical Sciences, Geosciences, and Biosciences of the U.S. Department of Energy at Lawrence Berkeley National Laboratory under Contract No. DE-AC02-05CH11231. The curium-248 used in this work was supplied by the U.S. Department of Energy through the transplutonium element production facilities at ORNL.

*Corresponding author.
Electronic address: Kristina.Kvashnina@fysik.uu.se

[1] J. L. Sarrao, L. A. Morales, J. D. Thompson, B. L. Scott, G. R. Stewart, F. Wastin, J. Rebizant, P. Boulet, E. Colineau, and G. H. Lander, Nature (London) **420**, 297 (2002).
[2] S. Heathman, R. G. Haire, T. Le Bihan, A. Lindbaum, M. Idiri, P. Nomrmile, S. Li, R. Ahuja, B. Johansson, and G. H. Lander, Science **309**, 110 (2005).
[3] S. Butorin, J. Electron Spectrosc. Relat. Phenom. **110**, 213 (2000).
[4] S. M. Butorin, D. K. Shuh, K. Kvashnina, K. Ollila, Y. Albinsson, J.-H. Guo, L. Werme, and J. Nordgren (to be published).
[5] L. Pauling, *Nature of Chemical Bonding* (Cornell University Press, New York, 1939), p. 26.
[6] V. Milman, B. Winkler, and C. J. Pickard, J. Nucl. Mater. **322**, 165 (2003).
[7] S. Skanthakumar, C. W. Williams, and L. Soderholm, Phys. Rev. B **64**, 144521 (2001).
[8] P. Soderlind, O. Eriksson, B. Johansson, and J. M. Wills, Phys. Rev. B **61**, 8119 (2000); **50**, 7291 (1994).
[9] C. J. Packard, B. Winkler, R. K. Chen, M. C. Payne, M. H. Lee, J. S. Lin, J. A. White, V. Milamn, and D. Vanderbilt, Phys. Rev. Lett. **85**, 5122 (2000).
[10] E. Simoni, M. Louis, S. Hubert, and S. Xia, Opt. Mater. **4**, 641

(1995).
[11] Y. Mochizuki and H. Tatewaki, J. Chem. Phys. **116**, 8838 (2002).
[12] K. G. Dyall, I. P. Grant, and S. Wilson, J. Phys. B **17**, L45 (1984).
[13] Y. Mochizuki and H. Tatewaki, J. Chem. Phys. **118**, 9201 (2003).
[14] J. Sytsma, K. M. Murdoch, and N. M. Edelstein, Phys. Rev. B **52**, 12668 (1995).
[15] K. M. Murdoch, N. M. Edelstein, L. A. Boatner, and M. M. Abraham, J. Chem. Phys. **105**, 2539 (1996).
[16] K. M. Murdoch, A. D. Nguyen, and N. M. Edelstein, Phys. Rev. B **56**, 3038 (1997).
[17] M. Illemassene, N. M. Edelstein, K. M. Murdoch, M. Karbowiak, R. Cavellec, and S. Hubert, J. Lumin. **86**, 45 (2000).
[18] J. V. Beitz and J. P. Hessler, Nucl. Technol. **51**, 169 (1980).
[19] T. Kimura and G. R. Choppin, J. Alloys Compd. **213**, 313 (1994).
[20] J. Sugar, Phys. Rev. B **5**, 1785 (1972).
[21] K. O. Kvashnina, S. M. Butorin, B. Hjörvarsson, J.-H. Guo, and J. Nordgren, AIP Conf. Proc. **837**, 255 (2006).
[22] T. Warwick, P. Heimann, D. Mossessian, W. McKinney, and H. Padmore, Rev. Sci. Instrum. **66**, 2037 (1995).
[23] J. Nordgren and R. Nyholm, Nucl. Instrum. Methods Phys. Res. A **246**, 242 (1986).
[24] J. Nordgren, G. Bray, S. Cramm, R. Nyholm, J-E Rubensson, and N. Wassdahl, Rev. Sci. Instrum. **60**, 1690 (1989).
[25] *Giant Resonances in Atoms, Molecules and Solids*, edited by J. P. Connerade, J. M. Esteva and R. C. Karnatak (Plenum, New York, 1987).
[26] R. D. Cowan, *The Theory of Atomic Structure and Spectra* (University of California Press, Berkeley, 1981).
[27] S. Butorin, J. Electron Spectrosc. Relat. Phenom. **110**, 235 (2000).
[28] S. M. Butorin, C. Sathe, A. Agui, F. Saalem, J. A. Alonso, and J. Nordgren, Solid State Commun. **135**, 716 (2005).
[29] W. Cao and L. E. Cross, Phys. Rev. B **44**, 2169 (1991).
[30] D. W. Lynch and R. D. Cowan, Phys. Rev. B **36**, 9228 (1987).
[31] M. Richter, M. Meyer, M. Pahler, T. Prescher, E. v. Raven, B. Sonntag, and H.-E. Wetzel, Phys. Rev. A **40**, 7007 (1989).
[32] H. Ogasawara, A. Kotani, and B. T. Thole, Phys. Rev. B **50**, 12332 (1994).